JOURNAL OF GEOPHYSICAL RESEARCH, VOL. 102, NO. D24, PAGES 29,475–29,482, DECEMBER 26, 1997

Seasonal change in understory reflectance of boreal forests and influence on canopy vegetation indices

John R. Miller,[1] H. Peter White,[1] Jing M. Chen,[2] Derek R. Peddle,[3] Greg McDermid,[4] Richard A. Fournier,[5] Paul Shepherd,[6] Irene Rubinstein,[6] Jim Freemantle,[6] Raymond Soffer,[6] and Ellsworth LeDrew[4]

Abstract. One objective of the Boreal Ecosystem-Atmospheric Study (BOREAS) is to increase our understanding of the nature of canopy spectral bidirectional reflectance in the visible/near-infrared regimes for open canopies typical of boreal forest stands. For such stands, the need to characterize the reflectance of the sunlit and shaded vegetated understory is critical. These variables are subject to temporal variability due to differences in species phenology and foliar display as well as diurnal and seasonal changes in solar illumination through a seasonally varying upper canopy foliar area. To provide for this need, a multiteam field effort was mounted to measure the nadir midday understory reflectance for the flux tower sites during 1994 BOREAS field campaigns between February and October, specifically during the winter focused field campaign (FFC-W), the spring thaw focused field campaign (FFC-T), and the three intensive field campaigns (IFC-1, IFC-2, and IFC-3) between June and September, which sample vegetation phenological change. This was accomplished by measuring at near-solar noon the sunlit and shaded nadir reflectance of the understory along a surveyed leaf area index (LAI) transect line at each flux tower site. Site-to-site comparisons of understory reflectance spectra reveal stand differences that become more significant as the season progresses. Mean midday understory reflectance spectra were observed to be remarkably consistent over the season for young jack pine stands, followed by somewhat increased variability for mature jack pine, and significant seasonal variability for black spruce stands. Derived vegetation indices for understories are generally consistent with extrapolations of previous relationships of canopy spectral vegetation indices (VIs) versus leaf area index to zero LAI. Inclusion of these "zero-LAI" understory-derived indices significantly enhance the correlation in the linear VI-LAI relationships.

1. Introduction

Vegetation indices (VI) are considered a means of deriving canopy biophysical variables such as leaf area index (LAI), percent green cover, and fractional absorption of photosynthetically active radiation (FPAR) [e.g., *Sellers*, 1985, 1987; *Choudhury*, 1987; *Hall et al.*, 1992], in spite of a number of documented inherent problems [e. g., *Baret and Guyot*, 1991; *Myneni et al.*, 1995]. The global mapping of canopy biophysical variables as data products in the Earth Observing System era is premised on strategies to select or interpret a variety of VIs so as to minimize the potentially confounding influences of the atmosphere, soil or understory, view-Sun angles, topography, clouds, and shadow [*Running et al.* 1994]. Significant progress has been made to deal with many of these factors using variants of VIs or through inverse modeling-based approaches. In particular, the influence of shadow and bidirectional reflectance properties for conifer forest stands is being approached through models [*Li and Strahler*, 1985; *Schaaf et al.*, 1994] and through BRDF field data [*Deering et al.*, 1994]. For the influence of soil understory for crop and semi-arid canopies, modified VIs are promising [*Qi et al.*, 1994; *Huete and Liu*, 1994].

The boreal forest canopies pose special challenges, however, with respect to understory effects on the above-canopy reflectance properties for sparse or open conifer canopies. In the northern boreal forests the understory is composed of mixtures of lichens, mosses, and short herb species which are not spectrally distinct from the overstory canopy, unlike the previously studied cases for canopies over soils [e. g., *Richardson and Wiegand*, 1990]. In the BOREAS project, conifer sites are dominated by black spruce (*Picea mariana*) or jack pine (*Pinus banksiana*), with additional contributions by aspen (*Populus tremuloides*) in mixed stands, each accompanied with specific understory species types [*Halliwell and Apps*, 1996; *Bubier et al.*, this issue]. Previous spectral reflectance measurements of vegetated understory components are limited to laboratory studies of mosses [*Vogelmann and Moss*, 1993; *Bubier et al.*, this issue] and field measurements of subarctic lichens [*Petzold and Goward*, 1988] and landscape components in western Oregon forests [*Goward et al.*, 1994]. However, the boreal forest un-

[1]Department of Physics and Astronomy, York University, North York, Ontario, Canada.
[2]Canada Centre for Remote Sensing, Ottawa, Ontario, Canada.
[3]Department of Geography, University of Lethbridge, Lethbridge, Alberta, Canada.
[4]Department of Geography, University of Waterloo, Waterloo, Ontario, Canada.
[5]Natural Resources Canada, Canadian Forest Service, Sainte-Foy, Quebec, Canada.
[6]Institute for Space and Terrestrial Science, North York, Ontario, Canada.

Paper number 97JD02558.
0148-0227/97/97JD-2558$09.00

derstories are expected to show a temporal cycle in reflectance properties due to differences in species phenology and foliar display as well as diurnal and seasonal changes in solar illumination through a seasonally varying overstory canopy. Therefore the characterization of the seasonal behavior of the understory of each of the dominant boreal species to evaluate or develop methods of relating vegetation indices to canopy biophysical parameters was an essential part of the BOREAS experiment. The importance of this task is underscored because of an apparent dearth of such understory characterizations in the literature. Significant technical and logistical challenges must be overcome in field measurements which must cope with a complex spatial distribution of forest understory features, variable illumination conditions typically involving a combination of direct sunlight, sunflecks, penumbra and shade, as well as the demands of field measurements in relatively remote sites spanning the entire season.

The goals of this paper are to present a methodology for understory reflectance measurements, to document the seasonal change in the spectral reflectance associated with the understories of black spruce and jack pine boreal forest stands of this study, and to present a preliminary analysis of the role played by understory reflectance on the relationship between vegetation indices and LAI for these canopies, as an extension of previous work on these sites by *Chen and Cihlar* [1996].

2. Methods

2.1. Sites and Data Set

In this study, the seasonal change in the mean midday understory spectral reflectance was characterized at eight BOREAS flux tower sites, during five BOREAS field campaigns in 1994, spanning the period from February to September. In spite of some data gaps due to specific weather and scheduling difficulties, the data collected permit seasonal or stand-specific changes to be tracked. The timing of the five campaigns allows for the understory to be viewed as an evolving feature during one growing season. The campaigns are referred to as FFC-W (focused field campaign-winter) (February 1994), FFC-T (focused field campaign-thaw) (April 1994), IFC-1 (intensive field campaign 1) (May/June 1994), IFC-2 (July 1994), and IFC-3 (September 1994). Sites were visited at the northern study area (NSA) in northern Manitoba, Canada, near Thompson, and at the southern study area (SSA) in Saskatchewan, Canada, near Candle Lake. In northern (N) and southern (S) study areas the understories were observed at the following BOREAS flux tower sites: fen (NFEN, SFEN), old black spruce (NOBS, SOBS), old jack pine (NOJP, SOJP), and young jack pine (NYJP, SYJP). Initial attempts to obtain understory reflectance data at the SSA and NSA aspen sites were abandoned due to the complicating effect of the height of the dominant hazelnut undergrowth. A summary of the data sets obtained, the equipment used, the dates of acquisition, and the scientists leading the field efforts are provided in Table 1.

2.2. Determination of a Field Measurement Strategy

Our objective was to obtain an estimate of the average midday spectral reflectance of the understory for each field campaign in order to specify this boundary condition in canopy reflectance modeling or interpretation. Therefore the experimental design focused on (1) determination of an appopriate method of spatial averaging; (2) characterization of the spectral reflectance of the understory under direct sunlight (Sunfleck) and shadow illumination conditions; and (3) observations within 2 hours of local solar noon, so as to generate measurements of the understory reflectance factors relevant to midday remote sensing observations. Whereas understory reflectance characterization on a species basis is of interest, this would have required a substantially different measurement strategy and did not conform to the primary thrust of this study. Similarly, the characterization of the complete BRDF of the understory was considered outside the scope of this study.

2.3. Field Methodology

Nadir-viewing field spectrometers were used to measure the sunlit and shaded (where possible) understory reflectances at labeled positions at 10 m intervals along the surveyed LAI transect line [*Chen*, 1996a] at each flux tower site. This transect normally runs in a southeast direction from the flux tower at each site. At each marker location, a representative understory area was chosen as the observation target and the predominant illumination condition determined: direct-Sun illuminated (Sunfleck) or shade. At each location the spectrometer observations included (1) multiple measurements of reflected spectral radiance from the target vegetation, followed by (2) a measurement of the incident irradiance spectrum by viewing a standard reflectance panel suspended, horizontally (visually determined), 2 to 10 cm above the understory vegetation. The two sets of spectra were normally collected within 5–10 s to minimize the effects of Sunfleck change due to wind or atmospheric illumination changes. The panel measurements were corrected for known illumination anisotropy (i.e., due to solar zenith angle) before computation of the target bidirectional reflectance factor (BRF), using the BRF calibration coefficients of Kodak gray card or Spectralon panels as a standard reflectance panel [*Soffer et al.*, 1995]. Spectral reflectance was calculated as the ratio of the dark-current corrected spectrometer signals for the target divided by that for the panel, multiplied by the panel BRF coefficient. Additional details on the field measurements and the data processing are provided by *White et al.* [1995] and *Peddle et al.* [1995]. Observations at 10–40 individual understory locations along the 100–300 m LAI line at each flux tower site permitted the calculation of a mean midday reflectance at the site. An exception to this methodology was adopted during IFC-2 where measurements were species specific but accompanied by coverage aerial estimates of these species as noted by the field experimenter, thereby allowing weighted-average understory reflectance spectra to be determined and reported here.

In addition to the computation of mean midday spectral reflectance factors for the understory, the values of particularly relevant vegetation indices (VIs) for this study were also calculated from the measured values of BRF by averaging over spectral regions defined by Landsat Thematic Mapper bands 3 and 4 to give reflectance values near 680 nm (denoted r_{red}) and near 800 nm (denoted r_{NIR}). The vegetation indices selected were the simple ratio (SR) [*Jordan*, 1969], normalized difference vegetation index (NDVI) [*Rouse et al.*, 1974], and the modified simple ratio (MSR) [*Chen*, 1996b]. These indices are defined as

$$\mathrm{SR} = \frac{r_{\mathrm{NIR}}}{r_{\mathrm{red}}}; \quad \mathrm{NDVI} = \frac{(r_{\mathrm{NIR}} - r_{\mathrm{red}})}{(r_{\mathrm{NIR}} + r_{\mathrm{red}})}; \quad \mathrm{MSR} = \frac{\mathrm{SR}-1}{\sqrt{\mathrm{SR}+1}} \qquad (1)$$

Table 1. Summary of Understory Reflectance Data Set Acquisition Attributes

Field Campaign[a]	Study Area[b]	Site[c]	Instrument Used[d]	Panel Used[e]	Observation Date	Comment[f]	Observers[g]
FFC-W	NSA	fen	SE590	KGC-W	12-Feb.-94	Sun/debris	IR, JF
		OJP	SE590	KGC-W	12-Feb.-94	shade	IR, JF
		YJP	SE590	KGC-W	12-Feb.-94	shade	IR, JF
	SSA	fen	SE590	KGC-W	09-Feb.-94	Sun	RS, IR, JF
		OBS	SE590	KGC-W	08-Feb.-94	Sun/shade	RS, IR, JF
		OJP	SE590	KGC-W	06-Feb.-94	Sun/shade	RS, IR, JF
		YJP	SE590	KGC-W	09-Feb.-94	Sun/shade	RS, IR, JF
FFC-T	NSA	fen	ASD	KGC-W	21-April-94	Sun(s, v)	DP, GM
		OJP	ASD	KGC-W	21-April-94	Sun/shade(s)	DP, GM
	SSA	OBS	ASD	KGC-W	16-April-94	Sun/shade(s, v)	DP, GM
		OJP	ASD	KGC-W	17-April-94	Sun/shade(v)	DP, GM
		YJP	ASD	KGC-W	17-April-94	Sun/shade(v)	DP, GM
IFC-1	NSA	OJP	SE590	KGC-W	11(13)-June-94	Sun/shade	JC
	SSA	OBS	SE590	KGC-W	31-May-94	Sun/shade	PS
		OJP	SE590	KGC-W	26-May-94	Sun/shade	PS
		YJP	SE590	KGC-W	26-May-94	Sun/shade	PS
IFC-2	NSA	OBS	SE590	KGC-W	16-July-94	Sun/shade	RF
	SSA	OBS	SE590	KGC-W	23-July-94	Sun/shade	RF
		OJP	SE590	KGC-W	21-July-94	Sun/shade	RF
		YJP	SE590	KGC-W	20-July-94	Sun/shade	RF
IFC-3	NSA	fen	SE590	KGC-G	03-Sept.-94	Sun	HPW, JC
		OBS	SE590	KGC-G	02-Sept.-94	Sun/shade	HPW, JC
		OJP	SE590	KGC-G	06(07)-Sept.-94	Sun/shade	HPW, JC
		YJP	SE590	KGC-G	01-Sept.-94	Sun/shade	HPW, JC
	SSA	fen	SE590	KGC-G	12-Sept.-94	Sun/shade	HPW, JC
		OBS	SE590	KGC-G	13-Sept.-94	Sun/shade	HPW, JC
		OJP	SE590	KGC-G	12-Sept.-94	Sun/shade	HPW, JC
		YJP	SE590	KGC-G	12(13)(16)-Sept.-94	Sun/shade	HPW, JC

[a]Field campaign, which BOREAS campaign was under way during the observation.
[b]Study area at which the flux tower site was located SSA, southern study area (near Candle Lake, Saskatchewan). NSA, northern study area (near Thompson, Manitoba).
[c]Flux tower site observed: fen, marsh/swamp; OBS, old black spruce; OJP, old jack pine; YJP, young jack pine.
[d]Instrument used for the measurements. ASD, analytic spectral devices, University of Waterloo; SE590, Spectron Engineering, York University.
[e]Standard (calibrated) reflectance panel used as a reference. KGC-W, white side of a Kodak gray card; KGC-G, gray side of a Kodak gray card [*Soffer et al.*, 1995].
[f]Understory conditions at time of observation. Sun, target illumination contained no (or minimal) shadowing; shade, target illumination contained no (or minimal) influence of Sun flecks. (s), snow was observed (default for FFC-W); (v), Vegetation was observed (default for all IFCs).
[g]People involved in the actual field data-collection process in the field. IR, Irene Rubinstein; JF, Jim Freemantle; RS, Raymond Soffer; DP, Derek Peddle; GM, Greg McDermid; JC, Jing Chen; PS, Paul Shepherd; RF, Richard Fournier; HPW, Peter White.

3. Results and Discussion

3.1. Variation of Midday Understory Spectral Reflectance Between Conifer Stands by Campaign

With the northern and southern study areas separated by some 600 km, climate differences represented by differences in local temperature and moisture cycles are expected to find expression in the understory development and therefore reflectance for each of the five field campaigns between February and October. BOREAS experiment details are presented by *Sellers et al.* [1995]. The first series of graphs, presented as Figures 1–5, show the mean midday understory reflectances on a campaign by campaign basis. In each graph the number of understory spectral observations used to determine the mean spectrum is indicated in parentheses in the legend; in addition, the standard error of the mean (SE = variance/$\sqrt{n}$) is indicated at 50 nm intervals to provide a measure of the confidence in the mean spectrum and the variability encountered in the understory composition along the observation track.

3.1.1. FFC-W understory spectra. February's campaign (FFC-W) allowed measurements to be made of the sunlit snow-covered understory at most BOREAS SSA sites, albeit at daytime temperatures as low as −35°C, and consequently yielding small sample sizes (<6), except for NYJP and SFEN. At NSA, only the fen site provided any sunlit data. However, since observations of shade understory snow at other sites provided reflectance spectra, similar to sunlit spectra both in shape and in magnitude, within one standard error, snow reflectance spectra obtained in shade are also reported here for other NSA sites. A comparison of all FFC-W snow understory reflectance spectra are provided in Figure 1. In all cases there is a decrease in derived mean sunlit understory reflectance at wavelengths greater than 850 nm, a common feature observed in all snow reflectance regardless of the snow properties [*Warren and Wiscombe*, 1980]. The "flat plateau" between these wavelengths are mildly indicative of both low illumination angles (>70° solar zenith angles) and small snow grain size. The presence of impurities in the snow cover (surface debris, dormant and dead understory visible below the snow, etc.) may also account for the overall low (<0.8) reflectance observed in the southern conifer sites. The northern sites all have reflectance spectra ~20% higher than southern conifer sites.

3.1.2. FFC-T midday understory spectra. Sunlit snow was also observed in the understory of some sites during the thaw campaign in April. Similar features are observed, as

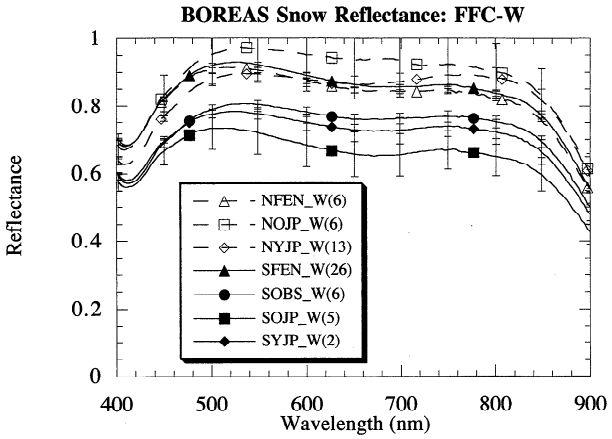

Figure 1. Mean midday sunlit understory (snow) reflectances for BOREAS sites during campaign FFC-W. Number in parentheses in the legend indicates the number of sample reflectance spectra used to produce the mean. Standard errors of the mean are indicated by the error bars at 50 nm intervals.

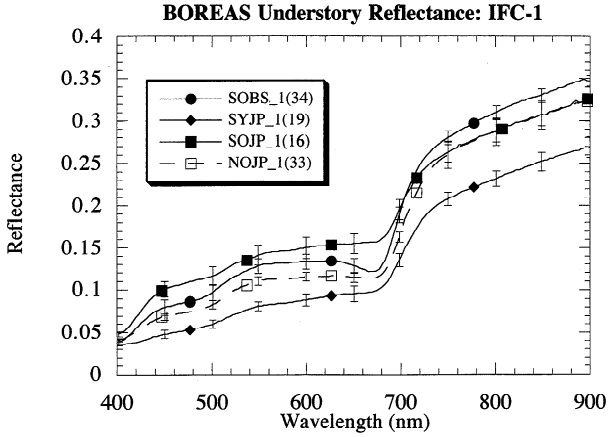

Figure 3. Mean midday sunlit understory reflectances for BOREAS sites during campaign IFC-1. Number in parentheses indicates the number of sample reflectance spectra used to produce the mean. Standard errors of the mean are indicated by error bars at 50 nm intervals.

shown in Figure 2, with a slightly greater decrease in reflectance at wavelengths beyond 800 nm and reflectance plateaus consistently below 0.8.

With snowmelt well under way during FFC-T at SSA, areas of exposed understory were also observed. As vegetation was observed in many sites during the fall campaign, a useful comparison can be made with the understory vegetation as observed in the early growing season at many of the sites. As observed throughout the summer campaigns, the OBS understory dominated by mosses (see *Bubier et al.* [this issue] for a detailed description) shows a more prominent chlorophyll absorption minimum (near 675 nm) than observed at other sites. As well, the OJP understory, dominated by lichen (*cladina stellaris*), is distinctive at visible wavelengths with its sharp reflectance increase between 420 and 440 nm and weak chlorophyll minimum. This early part of the growing season also shows a "rounded" NIR reflectance curve, peaking at ~800 nm. This feature has been observed in other types of vegetation stands when the soil substrate is dark and moist (causing a decrease in NIR reflectance, especially in the region of the water absorption feature beyond 900 nm) and contains dead and composting vegetation (causing an increase in red reflectance) [*Hardisky et al.*, 1984]. Observed shaded understory (both snow and vegetation) were indistinguishable from the derived sunlit reflectance spectra, within one standard error. The large range in understory reflectance spectra during the FFC-T campaign is clearly demonstrated in Figure 2, associated with snowmelt aerial spatial patterns.

3.1.3. IFC-1 midday understory spectra. The understory reflectance measurements during IFC-1 were obtained at the OJP site at NSA and at all three conifer sites at SSA, as shown in Figure 3. The YJP site provided the lowest sunlit reflectance coefficients when compared to the OJP and OBS sites. The OBS site showed a lower visible and a higher NIR reflectance relative to OJP. Spectral features associated with chlorophyll absorption were more pronounced in the OBS as compared to the other sites during all field campaigns.

Similarities in the shape of the understory reflectance spec-

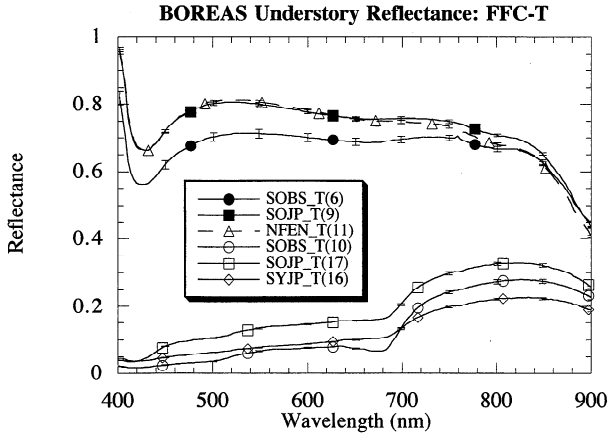

Figure 2. Mean midday sunlit understory (snow and vegetation) reflectances for BOREAS sites during campaign FFC-T. Number in parentheses indicates the number of sample reflectance spectra used to produce the mean. Standard errors of the mean are indicated by the error bars at 50 nm intervals.

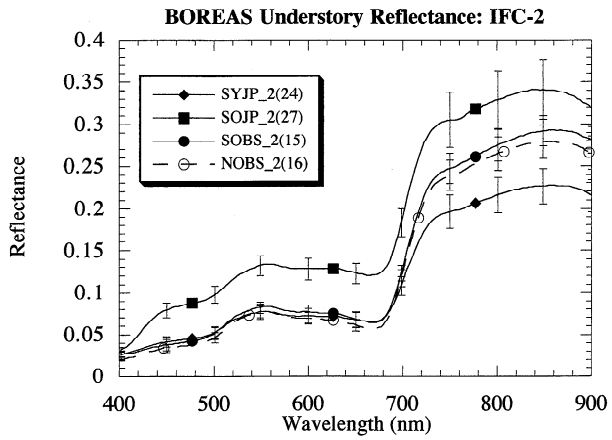

Figure 4. Mean midday sunlit understory reflectances for BOREAS sites during campaign IFC-2. Number in parentheses indicates the number of sample reflectance spectra used to produce the mean. Standard errors of the mean are indicated by error bars at 50 nm intervals.

tra were observed for the mature and young jack pine stands (OJP and YJP) as shown in Figure 3, with an ~10% offset between the two curves (OJP > YJP). The reflectance offset is qualitatively consistent with the observed larger aerial coverage of the understory with fallen tree trunks, dead needles, and exposed soil at the YJP sites, with similar understory vegetation components. OJP was more uniformly covered by lichen (primarily *cladina mitis*) [*Halliwell and Apps*, 1966] with less green vegetation (e.g., blueberry, cranberry) (see *Halliwell and Apps* [1966] for detailed occurrence tabulation) compared to YJP. Comparisons between the two study areas during this IFC are limited to the OJP understory, with the southern site presenting a slightly increased visible reflectance curve but equal NIR reflectance spectra at this time.

One trend viewed in all of the IFC-1 results is the continual increase in reflectance spectra in the NIR region. This tendency has been observed previously in situations when dry, dead plant material is common [*Elvidge*, 1990], and in cases of nitrogen enrichment in the soil [*Hardisky et al.*, 1984], although this condition was not observed again in our study. This NIR trend was also observed in the understory reflectance spectra taken at the NSA OJP and YJP sites (I. Supronowicz, Laval University, unpublished data, 1995) in early July (between IFC-1 and IFC-2), indicating that this feature is not unique to the IFC-1 period of the growing season.

3.1.4. IFC-2 midday understory spectra. Site measurements for NSA made during IFC-2 were limited due to logistical field operation constraints, whereas the three conifer sites in the south were visited. As shown in Figure 4, the YJP and OBS understory show similar visible spectra, with the OBS having a higher reflectance in the NIR region. All sites show the reemergence of the rounded NIR feature seen during FFC-T but not so pronounced.

Understory spectra at the two black spruce sites were equivalent during IFC-2. When comparing the understories of the jack pine sites during IFC-2, the reflectance spectral curves were observed to have the same general shape and features, with ~8% higher visible reflectance and twice that in NIR for OJP versus YJP.

3.1.5. IFC-3 midday understory spectra. Midday understory reflectance spectra for IFC-3 at all eight BOREAS flux tower sites are shown in Figure 5. A large range in understory reflectances is observed during IFC-3 with the largest differences occurring in the NIR region. Patterns of differences between dominant-species stands or between northern and southern areas are not so easily discernible for this IFC. In the north, similarities are observed in the visible spectra for the OJP and OBS sites, each with a 650 nm region chlorophyll absorption feature and a 500–600 nm reflectance peak, unlike the YJP and fen sites. A simple offset between OJP to YJP reflectance curves are not observed. Larger NIR reflectance was observed in the northern OJP than in the southern OJP because the northern OJP was wetter, yielding more green vegetation (blueberry, cranberry, etc.).

Comparisons in the southern study area mimic those made during other IFCs, with OBS showing more predominant features at ~650 nm and in the 500–600 nm region, and the two jack pine sites showing very similar curves with an apparent offset between them.

Northern to southern region comparisons can be made for all canopy sites during this field campaign. While the fen sites differed in water content (more surface water existing in the southern site), Figure 5 shows them both to have similar shapes

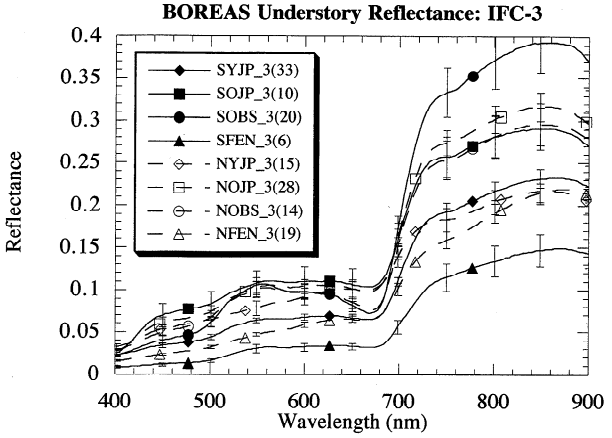

Figure 5. Mean midday sunlit understory reflectances for BOREAS sites during campaign IFC-3. Number in parentheses indicates the number of sample reflectance spectra used to produce the mean. Standard errors of the mean are indicated by error bars at 50 nm intervals.

and spectral features. The northern (drier) site, however, has a consistently higher (by a factor of ~1.5) reflectance coefficient at all observed wavelengths. For OBS, both study areas provided very similar visible reflectance curves. The southern OBS site however had a NIR reflectance notably higher than that derived for the north (again by a factor of ~1.5). Both the old and the young jack pine sites had very similar reflectance spectra between study areas (within 1 standard error) during this field campaign.

3.2. Seasonal Variation in Midday Understory Reflectance for Each Conifer Site

Since a fixed association can be drawn between overstory conifer species and the understory dominant species based on moisture regimes [*Halliwell and Apps*, 1996; *Bubier et al.*, this issue], it is important to determine the degree of seasonal variation in the mean midday understory reflectance. Some variation might be expected with understory foliar phenology, species proportion changes, as well as changes in leaf size, leaf color, or production of flowers, seeds, or berries. The seasonal change observed from April to September in the mean midday understory reflectance spectra for YJP, OJP, and OBS sites is presented in Figures 6, 7, and 8, respectively.

The understory spectra for the young jack pine site in Figure 6, with its emphasis on the southern site, shows remarkable consistency over the entire early spring to fall period. The seasonal variation is largely restricted to the chlorophyll absorption region between 600 and 680 nm, with the lowest reflectance in this wavelength region observed in the south during IFC-2 and IFC-3. Presumably, the consistency between spectra can be largely attributed to the dominant role played by branch litter at BOREAS YJP sites.

The seasonal variation in the understory mean midday reflectance spectra for mature jack pine, as shown in Figure 7, is larger than for young jack pine stands. The variability in spectral observations at individual sites is somewhat larger, as indicated by standard errors, with separability being statistically significant only in the chlorophyll absorption region. Therefore this study suggests that a fixed OJP understory reflectance spectrum can be assumed with small errors, except for the red region.

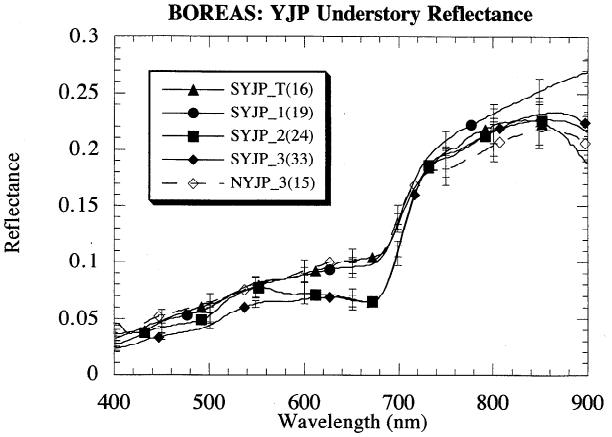

Figure 6. Mean midday sunlit understory reflectances for young jack pine (YJP) sites, northern (N) and southern (S) study areas, during the 1994 BOREAS campaigns. Number in parentheses indicates the number of sample reflectance spectra used to produce the mean. Standard errors of the mean are indicated by error bars at 50 nm intervals.

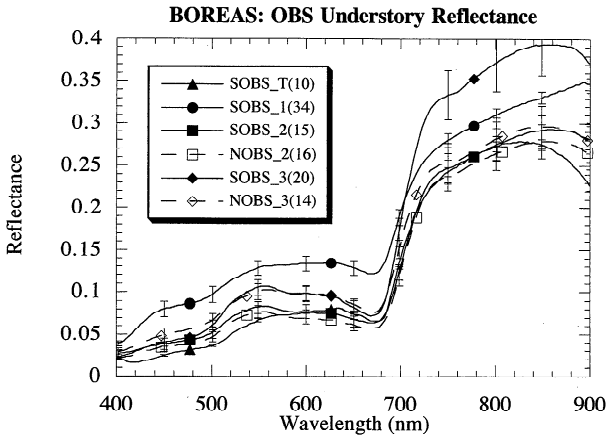

Figure 8. Mean midday sunlit understory reflectances for old black spruce (OBS) sites during the 1994 BOREAS campaigns. Number of sample reflectance spectra used to produce the mean are indicated in parentheses. Standard errors of the mean are indicated by error bars at 50 nm intervals.

Seasonal variation for OBS understory spectra, shown in Figure 8, indicates relatively large differences, both in the visible and in the near-infrared regions. The most significant departure in the visible region is observed in southern black spruce in June, while the most significant departure in the near infrared is observed in the southern black spruce site in September. Such variations are consistent with changes in moisture levels and/or moss species dominance [*Bubier et al.*, this issue]. Figure 8 clearly illustrates the relatively large variability in the understory reflectance associated with wet black spruce sites, although further work will be required to determine whether this is phenology based or moisture based.

3.3. Understory Vegetation Indices and Their Implication on VI-LAI Relationships

The seasonal variation and stand variation in the vegetation indices (VI), such as the simple ratio (SR), normalized difference vegetation index (NDVI), and the modified simple ratio (MSR) can readily be derived from the BOREAS understory midday reflectances from this study; the seasonal/stand variation in the most basic VI, the simple ratio (SR), is shown as an illustration in Figure 9. The seasonal trends of these indices for the fen and jack pine stand types show an increase in VI values from the early spring to midsummer period, followed by a plateau in the late summer (suggested for NSA data and demonstrated for SSA). Black spruce sites do not show such a regular seasonal trend. These understory VI trends have their most significant implication in the potential to alter the satellite-observed VI for the sparse boreal canopies.

Chen and Cihlar [1996] have reported NDVI, SR, and MSR indices derived from Landsat-TM imagery (after correction for atmospheric effects) for a variety of BOREAS jack pine and black spruce sites during IFC-1 and IFC-2 to evaluate the efficacy of a number of VI-LAI relationships. As indicated in Table 2, such relationships are relatively weak (low r^2) when derived on a per species basis due to the small range of LAI values associated with the overstory canopies at BOREAS and the perturbing influence of the understory on the satellite-observed optical signal. If one imagines the decrease in LAI

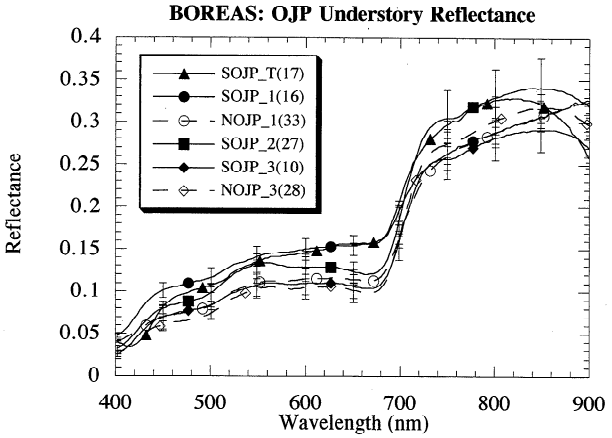

Figure 7. Mean midday sunlit understory reflectances for old jack pine (OJP) sites, northern (N) and southern (S) study areas, during the 1994 BOREAS campaigns. Number in parentheses indicates the number of sample reflectance spectra used to produce the mean. Standard errors of the mean are indicated by error bars at 50 nm intervals.

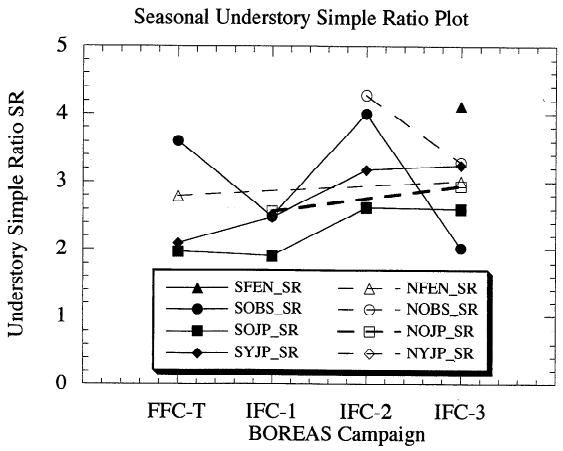

Figure 9. Seasonal change in the vegetation index, simple ratio (SR), for the understory at BOREAS sites during 1994.

being accomplished by removal of trees in a stand, with a fixed understory composition, then the satellite-derived VI would be increasingly influenced by the understory until at zero LAI the VI value should simply be that of the understory. This is clearly an idealized case because significant changes in the overstory canopy coverage would likely result in departures in composition of the understory from that observed in actual under-canopy measurements. The extrapolation of the TM-derived VI-LAI relationships to zero LAI in Figure 10 (shown by dashed lines) in most cases is representative of the understory reflectance-derived Vl values. However, in some cases, VI intercepts at zero LAI provide nonrealistic, even negative results (not shown here). If the understory VI observed at BOREAS is considered part of the VI-LAI relationship, that is the zero-LAI datum, the accuracy of all VI-canopy-parameter relationships is seen to improve considerably. As seen in Table 2, compared to linear VI-LAI regressions that do not include this datum, the recalculated VI-LAI regression, with the zero-LAI indices included, results in correlation coefficient (r^2) values increasing from between 0.46 and 0.95 to between 0.74 and 0.99.

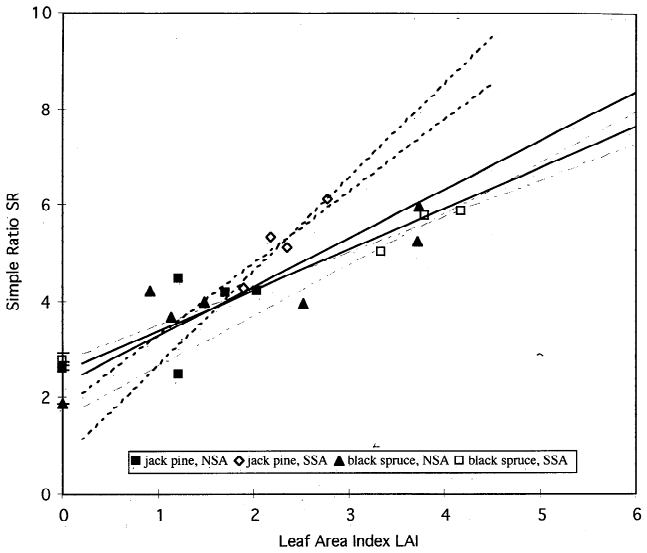

Figure 10. Relationships for BOREAS campaign IFC-1 between stand vegetation index simple ratio (SR) from Landsat-TM and field-measured above-canopy LAI for BOREAS jack pine and black spruce sites [after *Chen and Cihlar*, 1996a], derived with and without the understory "zero-LAI" datum: jack pine, SSA data, is indicated by two dashed lines; jack pine, NSA, is indicated by two solid lines, and black spruce, SSA, is indicated by two dashed-dotted lines. For each pair of lines, one will intersect the associated understory zero-LAI data point used in the regression fit.

4. Conclusions

BOREAS sites have shown a definite and observable seasonal variation in the sunlit mean understory reflectance spectra in the visible/NIR regions as a function of species-dominant forest stands. These have been documented for black spruce and young versus mature jack pine homogeneous stands. The differences between the understory reflectances for these stands appears to become more pronounced as the season progresses. This suggests that effort should be made to associate understory with stand type, especially later in the season, in future satellite data interpretation methodologies that attempt to uncouple the understory effects from apparent canopy reflectance for boreal forests.

Measurements of the seasonal variation (April to September) in the midday mean understory reflectance associated with each of the three BOREAS conifer stands revealed that seasonal variability was characteristic of stand type and was observed to increase by species in the following order: young jack pine (YJP), old jack pine (OJP), and old black spruce (OBS). YJP understory spectra were remarkably consistent throughout the season, whereas OJP understory spectra showed more seasonal variation over the entire visible to near-infrared region; for both YJP and OJP understory spectra, statistically significant differences were restricted to the chlorophyll absorption region (600–680 nm). The largest seasonal variations were observed in OBS understory reflectance spectra. However, since differences observed in the visible were not necessarily correlated to those in the near-infrared regions, more research is suggested to determine whether moss phenology and/or moisture regimes are responsible for the observed variability. The results suggest that the jack pine sites may reasonably be represented by seasonally independent understory reflectance spectra without serious error introduced in inverse canopy modeling. Understory reflectances from northern conifer sites were not distinguished from same-species southern sites, possibly due to the small number of measurements at the northern sites.

The vegetated understory in the sparse boreal conifer forests have been shown in this study to exhibit vegetation indices that are lower but fall within a similar range to overstory canopies. These understory indices (e. g., SR) are generally consistent with the "zero-LAI" extrapolations of satellite-derived VI-LAI relationships of *Chen and Cihlar* [1996a]. The use of observed understory reflectance spectra for "zero-LAI" indices resulted in a significant improvement (r^2) in the VI-LAI relationships over that derived from satellite data alone. To the extent that this understory data set is typical of the boreal forest ecosystem, this approach may provide a useful basis for accounting for the influence of understory in the development of relationships between other observations of satellite-derived vegetation indices and corresponding overstory canopy biophysical parameters.

Table 2. Linear Least Squares Fits to TM-Derived VI Data and BOREAS LAI Data [*Chen*, 1996a]. Including and Excluding the Understory VI Values From This Study

Sites	NDVI - LAI With (Without) Understory	MSR - LAI With (Without) Understory	SR - LAI With (Without) Understory
NOBS			
r^2	0.74 (0.61)	0.87 (0.46)	0.78 (0.68)
b	0.0388 (0.0344)	0.214 (0.203)	0.866 (0.852)
a	0.611 (0.624)	1.36 (1.40)	3.97 (4.02)
SOBS			
r^2	0.99 (0.95)	0.91 (0.66)	0.86 (0.66)
b	0.0278 (0.0436	0.151 (0.242)	0.592 (1.057)
a	0.626 (0.559)	1.45 (1.06)	4.33 (2.35)
SOJP			
r^2	0.95 (0.62)	0.91 (0.66)	0.86 (0.66)
b	0.154 (0.103)	0.505 (0.502)	1.50 (1.95)
a	0.318 (0.439)	0.525 (0.529)	1.81 (0.74)

Fit equation: LAI = a + b* VI.

Acknowledgments. We gratefully acknowledge funding for this research from the Natural Sciences and Engineering Research Council of Canada through the Collaborative Special Projects program and from Technology Ontario via the Institute for Space and Terrestrial Science (ISTS).

References

Baret, F., and G. Guyot, Potentials and limitations of vegetation indices for LAI and APAR assessment, *Remote Sens. Environ.*, *35*, 161–173, 1991.

Bubier, J. L., B. N. Rock, and P. M. Crill, Spectral reflectance measurements of boreal wetland and forest mosses, *J. Geophys. Res.*, this issue.

Chen, J., Optically-based methods for measuring seasonal variation in leaf area index in boreal conifer stands, *Agric. For. Meteorol.*, *80*, 138–163, 1996a.

Chen, J., Evaluation of vegetation indices and a modified simple ratio for boreal application, *Can. J. Remote Sens.*, *22*, 229–242, 1996b.

Chen, J., and J. Cihlar, Retrieving leaf area index of boreal conifer forests using Landsat TM images, *Remote Sens. Environ.*, *55*, 153–162, 1996.

Choudhury, B., Relationships between vegetation indices, radiation absorption, and net photosynthesis evaluated by a sensitivity analysis, *Remote Sens. Environ.*, *22*, 209–233, 1987.

Deering, D. W., E M. Middleton, and T. F. Eck, Reflectance anisotropy for spruce-hemlock forest canopy, *Remote Sens. Environ.*, *47*, 242–260, 1994.

Elvidge, C.D., Visible and near infrared reflectance characteristics of dry plant material, *Int. J. Remote Sens.*, *11*, 1775–1795, 1990.

Goward, S. N., K. F. Huemmrich, and R H. Waring, Visible-near infrared spectral reflectance of landscape components in western Oregon, *Remote Sens. Environ.*, *47*, 190–203, 1994.

Hall, F. G., K. F. Huemmrich, K. F. Goetz, P. J. Sellers, and J. E. Nickeson, Satellite remote sensing of surface energy balance: Success, failures, and unresolved issues in FIFE, *J. Geophys. Res.*, *97*, 19,061–19,089, 1992.

Halliwell, D., and M. J. Apps, BOREAS biometry and auxiliary sites: Overstory and understory data, technical report, Can. For. Serv., North. For. Cent., Edmonton, Alberta, Canada, 1996.

Hardisky, M. A., F. C. Daiber, C. T. Roman, and V. Klemas, Remote sensing of biomass and annual net aerial primary productivity of salt marsh, *Remote Sens. Environ.*, *16*, 91–106, 1984.

Huete, A. R., and H. Q. Liu, An error and sensitivity analysis of the atmospheric- and soil-correcting variants of NDVI for the MODIS-EOS, *IEEE Trans. Geosci. Remote Sens.*, *32*, 897–905, 1994.

Jordan, C. F., Derivation of leaf area index from quality of light on the forest floor, *Ecology*, *50*, 663–666, 1969.

Li, X., and A. H. Strahler, Geometric-optical modeling of a conifer canopy, *IEEE Trans. Geosci. Remote Sens.*, *23*, 705–721, 1985.

Myneni, R. B., S. Maggion, J. Iaquinta, J. L. Privette, N. Gobron, B. Pinty, D. S. Kimes, M. M. Verstraete, and D. L. Williams, Optical remote sensing of vegetation: Modeling, caveats and algorithms, *Remote Sens. Environ.*, *51*, 169–188, 1995.

Peddle, D. R., H. Peter White, R. J. Soffer, J. R. Miller, and E. F. LeDrew, Reflectance processing of field spectrometer data in BOREAS, in *Proceedings of the 17th Canadian Symposium on Remote Sensing*, pp. 189–194, Can. Remote Sens. Soc., Can. Aeronaut. and Space Inst., Ottawa, 1995.

Petzold, D. E., and S. N. Goward, Reflectance spectra of subarctic lichens, *Remote Sens. Environ.*, *24*, 481–492, 1988.

Qi, J., A. Chehbouni, A. R. Huete, Y. H. Kerr, and S. Sorooshian, A modified soil adjusted vegetation index, *Remote Sens. Environ.*, *48*, 119–126, 1994.

Richardson, A. J., and C L. Wiegand, Comparison for two models for simulating the soil-vegetation composite of a developing cotton canopy, *Int. J. Remote Sens.*, *11*, 447–459, 1990.

Rouse, J. W., R. H. Haas, J. A. Schall, D. W. Deering, and J. C. Harlan, Monitoring the vernal advancement of retrogradation of natural vegetation, 371 pp., NASA/GSFC, Type III, final report, Greenbelt, Md., 1974.

Running, S. W., et al., Terrestrial remote sensing science and algorithms planned for EOS/MODIS, *Int. J. of Remote Sens.*, *15*, 3587–3620, 1994.

Schaaf, C. Barker, X. Li, and A. H. Strahler, Topographical effects on bidirectional and hemispheric reflectances calculated with a geometric-optical canopy model, *IEEE Trans. Geosci. Remote Sens.*, *32*, 1186–1193, 1994.

Sellers, P. J., Canopy reflectance, photosynthesis and transpiration, *Int. J. Remote Sens.*, *6*, 1335–1372, 1985.

Sellers, P. J., Canopy reflectance, photosynthesis and transpiration, II, The role of biophysics in the linearity of their dependence, *Remote Sens. Environ.*, *21*, 143–183, 1987.

Sellers, P., et al., The Boreal Ecosystem-Atmosphere Study (BOREAS): An overview and early results from the 1994 field year, *Bull. Am. Meteorol. Soc.*, *76*, 1549–1577, 1995.

Soffer, R. J., J. W. Harron, and J. R. Miller, Characterization of Kodak grey cards as reflectance reference panels in support of BOREAS field activities, in *Proceedings of the 17th Canadian Symposium on Remote Sensing*, pp. 357–362, Can. Remote Sens. Soc., Can. Aeronaut. and Space Inst., Ottawa, 1995.

Vogelmann, J. E., and D. M. Moss, Spectral reflectance measurements in the genus Sphagnum, *Remote Sens. Environ.*, *45*, 273–279, 1993.

Warren, S. G., and W. J. Wiscombe, A model for the spectral albedo of snow, II, Snow containing atmospheric aerosols, *J. Atmos. Sci.*, *37*, 2734–2745, 1980.

White, H. P., J. R. Miller, J. Chen, and D. R. Peddle, Seasonal change in mean understory reflectance for BOREAS sites: Preliminary results, in *Proceedings of the 17th Canadian Symposium on Remote Sensing*, pp. 189–194, Can. Remote Sens. Soc., Can. Aeronaut. and Space Inst., Ottawa, 1995.

J. M. Chen, Canada Centre for Remote Sensing, Ottawa, Ontario, K1A 0Y7, Canada.

R. A. Fournier, Natural Resources Canada, Canadian Forest Service, Sainte-Foy, Quebec, G1V 4C7, Canada.

J. Freemantle, I. Rubinstein, P. Shepherd, and R. Soffer, Institute for Space and Terrestrial Science, North York, Ontario, M3J 3K1, Canada.

E. LeDrew and G. McDermid, Department of Geography, University of Waterloo, Waterloo, Ontario, N2L 3G1, Canada.

J. R. Miller, and H. P. White, Department of Physics and Astronomy, York University, 4700 Keele Street, North York, Ontario M3J 1P3, Canada. (e-mail: miller@ed.ists.ca)

D. R. Peddle, Department of Geography, University of Lethbridge, Lethbridge, Alberta, T1K 3M4, Canada.

(Received April 29, 1996; revised August 4, 1997; accepted September 3, 1997.)